Iron and phosphorus dynamics in sediments from the western slope and deep basin of the Black Sea

Gijs Megens,

3363198

MSc Thesis

ECTS: 45

Supervisors:

Prof. dr. ir. C.P. Slomp

Dr. P. Kraal

Study:

Track: Environmental Geochemistry

Programme: Earth, Life and Climate

Department: Earth Sciences

Faculty: Geosciences

Utrecht University

Date:

March 17, 2015

Abstract

At present the Black Sea is the largest basin in the world with permanently anoxic deep waters and it has been anoxic for roughly the past 8000 years. The inflow of saline water from the Mediterranean through the Bosporus in what was until then an oxic, fresh-water, lacustrine environment led to a density driven stratification of the water column, which inhibits mixing. Consequently, the water column became divided between oxic surface waters and euxinic deep waters. This lake-marine transition influenced the phosphorus (P) and iron (Fe) speciation in the sediment. While P bearing Fe oxides were formed and preserved under the oxic lacustrine condition, the euxinic marine conditions instead favor the formation and preservation of FeS_2, which does not form a significant sink for P. At the same time, infiltration of HS^- into the lake sediment forms a sulfidization front above which Fe oxides are reduced by their reaction with HS^-, forming FeS and FeS_2 within the lacustrine deposits, releasing P into the porewater.

As P is an essential and often limiting nutrient and Fe oxides form an important sink for P, it is important to know how the Fe-P cycle is influenced by the interaction with HS^- and how this may affect P availability. Therefore, it is the aim of this study to determine the influence of the lake-marine transition and the sulfidization front on the sedimentary Fe and P record in the Black Sea. Furthermore, this paper aims to determine how sediments from the deep basin may differ from slope sediments in the Black Sea as a result of differences in sedimentation rates and the presence of an active Fe shuttle. In order to do so, two different cores collected during the 2013 PHOXY cruise on the R/V Pelagia are examined. One of the cores PHOX 4 was collected from the western slope (ca 400 mbss) of the Black Sea, the other (PHOX 12) from the deep basin (ca. 2000mbss). Both cores were subjected to total solid phase analysis, a sequential P extraction (SEDEX; Ruttenberg 1992) and two sequential Fe extractions (Claff et al., 2010 and Poulton and Canfield, 2005).

The data show that the lake-marine transition causes a shift in the importance of different sedimentary Fe and P pools. Where the oxic lacustrine system favored the preservation of Fe oxides and carbonates, the marine system favors the formation of FeS_2. The high concentrations of Fe and Fe-bound P in the surface sediments of both cores and of Fe oxides in PHOX 4 is the result of an Fe shuttle that transports Fe oxides and associated P from the shelf via the slope towards the deep basin of the Black Sea, undergoing continuous reduction via the reaction with HS^-. Furthermore, Organic Matter (OM), and consequently Org. P, is only preserved in the marine

environment, resulting in higher concentrations of org P in the marine sediments, compared to the lacustrine deposits, despite the anoxic conditions which favor the recycling of org P.

Additionally, the downward diffusion of HS^- into the lake sediments results in a replacement of Fe oxides that were previously present by FeS_2 through the reaction of Fe with HS^-. The PO_4^{3-} released as a consequence of the reduction of the Fe oxides by HS^-, diffuses upward and downward to below the S.F. were it can be react with Fe^{2+} in the porewater forming Fe-P minerals such as vivianite. As a result, enrichments in Fe-bound P are present below the S.F.

Table of Contents

1. Introduction

The widespread growth of hypoxic (<2 mL O2/L), anoxic (<0.2 mL O_2/L) or even euxinic (no oxygen; free sulfide) conditions in the water column in areas across the world, including the coastal zones,(Diaz and Rosenberg 2008) results in environmental ramifications, as it may, directly influence preservation of phosphorus (P) in the sediments and thereby its availability to biological processes. And as phosphorus is an essential, and often limiting, nutrient for marine primary production (Tyrell 1999), its behavior may directly influence the presence and extent of different marine biota.

The main input of new phosphorus into a marine system is from terrestrial sources through rivers (Froelich et al 1982; Meybeck 1982). As such, the potential regeneration of phosphorus from the sediment under euxinic conditions can become a major factor in the availability of phosphorus to biological processes (Delaney 1998; Ingall et al 1993). Consequently, the speciation of phosphorus in sediments and the stability of the different P pools are important.

In the water column, phosphorus is present primarily in the form of (di)hydrogen phosphate ($H_2PO_4^-$, HPO_4^{2-}), in which form it can be used by organisms in the formation of OM. There exist various potential sedimentary sinks for P which can decrease the amount of $H_2PO_4^-$and HPO_4^{2-} available in the water column. These sinks include (1) OM burial, (2) adsorption and precipitation of P with Fe (oxyhydr)oxides, Fe carbonates and clays, (3) burial of authigenic and biogenic Ca-bound P, including carbonate fluorapatite (CFA), and (4) deposition of carbonate ($CaCO_3$)-associated P (Froelich et al 1977).

Furthermore, sediment may contain detrital P from igneous or metamorphic origin, which is assumed to be deposited unaltered and its deposition, therefore, doesn't influence PO_4^{3-} concentrations in the water column (e.g. Ruttenberg 1992; Kraal et al 2012). The importance of the different P sinks (and potential sources), depends on the local depositional environment, which include redox conditions and sedimentation rates (Ingall et al 1993; Ingall et al 2005; Ruttenberg and Berner 1993).

As iron minerals, and especially Fe (oxyhydr)oxides can form an important sink for P in marine environments (Froelich et al. 1988; Ruttenberg and Sulak 2011), it is important to understand the behavior of iron under different conditions. Under oxic conditions Fe is deposited primarily in the form of Fe (oxyhydr)oxides and Fe carbonates. However, under euxinic conditions iron reacts with the hydrogen sulfide (HS^-), present in the porewater as a result of sulfate (SO_4^{2-}) reduction, forming iron monosulfide (FeS) and ultimately pyrite (FeS_2). As a consequence, the change from

oxic to euxinic conditions can release phosphorus from the sediment as Fe (oxyhydr)oxides are transformed into FeS_2 (Ingall and Jahnke 1997; Krom and Berner 1981; Krom and Sholkovitz 1978; Golterman 1995). Furthermore, Fe particles can be shuttled into the deep basin from the shelf and, as such, enrichment in Fe may occur in the basin (Lyons And Severmann 2006; Wijsman et al 2001, Scholz et al 2014). This may have a potentially strong influence on P burial in euxinic basins, as continuous shuttling of Fe oxides into the deep basin may result in the accumulation of the oxides in the sediment of the deep basin, if it is active in large enough quantities, and may thereby form a sink for P even in euxinic environments. (Jilbert and Slomp 2013).

An alternate path for the production of HS^- from SO_4^{2-}, aside from OM reduction, is through a reaction with CH_4 in a process called anaerobic oxidation of methane (AOM) (Eq. 1) (Barnes and Goldberg 1976; Reeburgh et al 1991). Recent studies propose additional pathways for AOM to occur, including by the usage of Fe oxides as an electron acceptor (Eq. 2)(Fe-mediated AOM) (Beal et al 2009; Egger et al 2015), as opposed to SO_4^{2-}, resulting in an additional method by which Fe oxides may be dissolved. Furthermore, Both pathways release bicarbonate (HCO_3^-), thereby potentially increasing the alkalinity of the system.

$$CH_4 + SO_4^{2-} \rightarrow HS^- + HCO_3^- + H2O \quad (1)$$

$$CH_4 + 8Fe(OH)_3 + 15H^+ \rightarrow HCO_3^- + 8Fe^{2+} + 21H_2O \quad (2)$$

Currently, the largest anoxic basin in the world is the Black Sea, where permanently euxinic conditions in the water ca 150 mbss. The inflow of saline water from the Mediterranean through the Bosporus, in combination with the riverine input of freshwater, leads to a density driven stratification of the water column, which inhibits mixing. As a consequence, the water column is divided in oxic surface waters and euxinic bottom waters (Eckert et al 2013). The sediment of the Black Sea is generally subdivided into three units (Ross et al 1970; Degens and Ross 1972), which are indicative of their depositional environment.

As a result of the melting of alpine and Scandinavian ice sheets during the end of the last glacial period (ca. 22-10 ka), riverine input of freshwater into the Black Sea basin was increased during this period. Simultaneously, the still prevalently low sea level prevented saline water from the Mediterranean from flowing through the Bosporus into the Black Sea. As a consequence, the Black Sea was an oxic freshwater lake environment during this period.(Degens and Ross 1972; Bahr et al. 2005). The sediments deposited during this interval are rich in carbonates and Fe oxides and are defined as Unit III (Ross et al 1970).

At ca. 9 ka, the sea level rise, induced by the global melting of the ice sheets form the last glacial period, resulted in the connection of the Black Sea with the Mediterranean, through the Bosporus (Ross et al 1970). This connection facilitated the inflow of saline waters from the Mediterranean into the previously freshwater Black Sea (i.e. the lake-marine transition). Subsequently, this caused stratification of the water column preventing effective mixing and inducing prevalent euxinic bottom water conditions (ca. 7.6 ka) (Eckert et al 2013). This change in depositional conditions induced by the inflow led to the formation of an OM-rich marine sapropel layer, as OM degradation was significantly slowed, due to the less efficient anaerobic degradation pathways. At the same time, anaerobic bacteria may favor enhanced primary production, as they are less effective at storing P and more effective at P cycling, than aerobic organisms. Consequently, organic P (Org. P) is potentially less efficient sequestered into the sediment. (Arthur and Dean 1998; Slomp et al 2002) The deposited sapropel layer (ca. 30 cm) is referred to as Unit II (Ross et al 1970; Degens and Ross 1972).

From ca. 2.7 ka onward (Eckert et al 2013), the carbonate exoskeletons of the coccolithophore *Emiliania huxleyi* are preserved in the sediments (Ross et al 1970; Degens and Ross 1972; Arthur and Dean 1998). The sediment, consisting of alternating thinly laminated layers of carbonate-rich and organic- and clay-rich layers, deposited during this interval is referred to as Unit I.

By investigating two different cores, one collected from the western slope and one from the deep basin of the Black Sea, this paper aims to determine (1) the influence of the lake-marine transition on the sedimentary Fe and P record, (2) the diagenetic influence of the prevalent euxinia of the system on the Fe and P pools and (3) the possible differences between slope and deep sediments.

2. Methods

For this study, two cores, retrieved from the western Black Sea during the 2013 PHOXY cruise with the *R/V Pelagia*, were analyzed. One core, with a length of 6 m was retrieved by gravity core at station PHOX 4 (43° 40.6’ N, 30° 7.5’E) (Fig. 1). This site, with a water depth of 377 m, is situated on the slope and features a relatively gentle incline, compared to the rest of the slope. It currently lies below the redoxcline (ca. 100-150 mbss). The other core was collected by piston core at station PHOX 12 (42° 56.2’ N, 30° 1.9’ E) (Fig. 1) and has a length of 10 m. With a water depth of 1969 m, the site is located in the deep basin and it features very little topography.

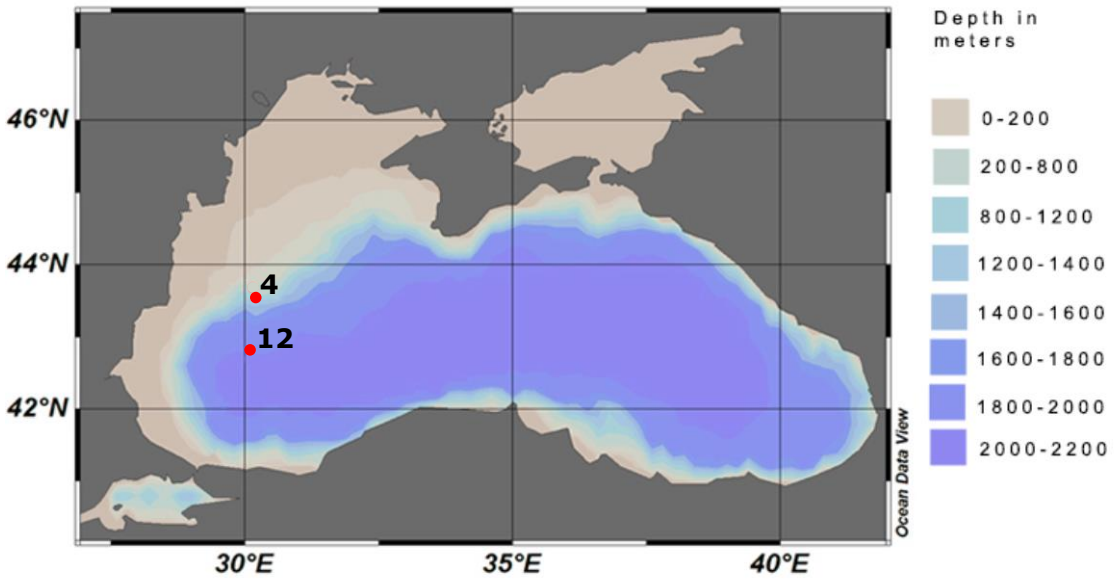

Figure 1. The approximate locations of PHOX 4 and PHOX 12 (cruise report PHOXY 2013).

2.1. Sampling

To prevent alteration of the sediment as a result of post-collection oxidation (Kraal et al 2009; Kraal and Slomp 2014), all sample handling and storage took place under anoxic conditions. For the solid phase analysis of the sediment of both cores 20 mL syringe samples were taken, sealed with parafilm and transferred to an anoxic glovebox, where they were transferred to PP/PE tubes. These were subsequently centrifuged at 4500 rpm for 30 min, after which the supernatant porewater was decanted and subsampled. The porewater was stored at 4°C. The solid phase in the greiner tubes was stored frozen (-20°C). On shore, the wet sediment was freeze-dried and ground in an agate mortar in an anaerobic chamber. A separate set of syringe samples was taken at lower resolution for the determination of porosity. (Cruise Report PHOXY 2013)

Separate 10 mL syringe samples were also collected for methane (CH_4) analysis, which were immediately transferred to glass bottles pre-filled with a saturated NaCl solution. The solution was, subsequently, topped of and the glass bottle sealed with a rubber stopper to negate the existence of air bubbles. The bottle was further closed with a screw cap and stored upside-down. On shore, 10 mL of nitrogen was added as headspace, prior to analysis. (Cruise Report PHOXY 2013)

A depth scale correction, based on the porewater profiles, has been applied to both PHOX 4 (30 cm) and PHOX 12 (20 cm) to account for the loss of surface material upon the core retrieval.

2.2. Porewater analysis

Subsamples of the porewater were filtered through 0.45 μm filters prior to analysis. HS^-, PO_4^{3-} and NH_4^+, among others, were analyzed on board via AutoAnalyzer. Analysis of S, Fe, Mn, trace metals, major elements took place on shore by ICP-OES, whereas SO_4^{2-} was analyzed by Ion Chromatography. The CH_4 samples were analyzed on shore using a Thermo Finnigan Trace GC gas chromatograph and a flame ionization detector. (Cruise Report PHOXY 2013)

2.3. Solid phase analyses

2.3.1. Total sediment composition

Approximately 0.125 g of the samples was dissolved overnight at 90°C in a closed Teflon bomb, using a mixture of 2.5 mL HF (40%) and 2.5 mL conc. $HClO_4/HNO_3$. The resulting solution was then evaporated at 160°C for ca. 3-4 h, until only a yellowish gel remained. Subsequently, the gel was redissolved overnight in 25mL 1M HNO_3, at 90°C. The resulting solution was then analyzed for total elemental concentrations using ICP-OES (Perkin Elmer optima 3000).

2.3.2. Organic carbon content

To determine the organic Carbon content, freeze-dried oxic subsamples were first decalcified, by dissolving ca. 0.2 g sample in 7mL 1 M HCl and constantly shaking (130 rpm) it for a period of ca. 4 h. Afterwards, the samples were centrifuged at 2300 rpm for 8 min and the resulting supernatant decanted. Subsequently, another 7 mL of 1 M HCl was added to the remaining sample and left to shake overnight. After another round of centrifugation and decantation of the supernatant, the remaining subsample was rinsed twice with UHQ and then oven dried for 48 h at 60°C, followed by grinding in an agate mortar. Approximately 10 mg of the treated samples was transferred to tin cups for analysis by a CN analyzer (Fisons Instruments NA 1500).

2.3.3. Sequential phosphorus extraction (SEDEX)

The P speciation was determined using the SEDEX method as developed by Ruttenberg (1992) and modified by Kraal et al (2010). This method separates the solid phase P into 5 pools (table 1): (1) exchangeable P, (2) Fe-bound P, (3) biogenic and authigenic calcium phosphate minerals, including CFA, and $CaCO_3$-associated P (Ca-bound P), (4) P associated with detrital material (det. P) and (5) OM associated P (org. P). All extractions (10 mL) took place within the span of a week and the samples were constantly shaken (120 rpm) during the extractions. The samples were flushed with argon during the addition of extractants for the first three extraction steps.

Table 1. The different pools targeted by the SEDEX extraction and the corresponding extraction solutions. The $MgCl_2$ solution was brought up to pH 8 using NaOH. The Na-acetate solution was buffered to pH 4 using acetic acid. * The CDB (citrate dithionite bicarbonate) extraction is the only step measured by ICP-OES, as opposed to the colorimetric method.

Step	Pool	Extraction solution	pH	time (h)
1	Exchangeable P	1M $MgCl_2$	8	0.5
2	Fe-bound P	CDB*	7.6	8
(wash)		1M $MgCl_2$	8	0.5
3	Ca-bound P	1M Na-acetate	4	6
(wash)		1M $MgCl_2$	8	0.5
4	Det. P	1M HCl	0	24
5	Org. P	Ashing (550°C)		2
		1M HCl	0	24

After filtration of the extracts through 0.45 μm filters, the P content in each extract was determined by colorimetry, except for the CDB solution, which was analyzed by ICP-OES, after dilution (5x) with UHQ. A molybdate-tartrate-sulfuric acid solution was used as a color reagent in the colorimetric analysis. Analysis, at a wavelength of 880 nm, took place approximately 15 min. after addition of the reagent.

2.3.4. Sequential iron extractions

Two different sequential extractions were used to analyze the Fe pools in the sediment. The first method, referred to here as Claff extraction, was adapted from Claff et al. (2010) and separates (1) labile Fe(II) and Fe(III), (2) crystalline Fe oxides and (3) pyrite. The second method, henceforth referred to as the Poulton extraction, was developed by Poulton and Canfield (2005) and distinguishes between (1) carbonate Fe (carb. Fe), including siderite and ankerite, (2) easily reducible Fe oxides, such as ferrihydrite and lepidocrocite, (3) reducible Fe oxides, including goethite, akaganéite and hematite and (4) magnetite. The pyrite extraction step described in Poulton's procedure was excluded. All extractions took place under constant agitation of the samples and the samples were flushed with argon during the addition of the extractants. The pools distinguished by each extraction method and the used procedures are shown in table 2.

Table 2. The different pools and corresponding extraction solutions as identified by the Claff and Poulton procedures. *CBD stand for citrate buffered dithionite.

Step	pool	Extraction solution	pH	time (h)
Claff				
1	labile Fe(II), Fe(III)	1 M HCl	1	4
2	Fe oxide	CBD*	4.8	4
3	Pyrite	Concentrated HNO_3		2
Poulton				
1	Carb. Fe	Na-acetate	4.5	24
2	easily red. Fe oxide	1M Hydroxylamine-HCl		24
3	Red. Fe oxide	CBD	4.8	2
4	Magnetite	NH_4-oxalate	3.2	6

After filtration of the extractants using 0.45 μm filters, the Fe content in each extract was determined via colorimetry, using a wavelength of 510 nm, except for the citrate buffered dithionite (CBD) extraction from Claff, which was determined via ICP-OES. A mixture of NH_4-acetate buffer (4 M NH_4-acetate / 14.4 M acetic acid) and 1,10-phenanthroline solution (1g/l phenanthroline / 2% v/v concentrated HCl) with a 1:2 ratio was used as an Fe trap. To ensure all Fe in the samples was present in the form of Fe(II) and, thereby, allow analysis of all Fe, a 100g/l hydroxyl-ammonium-chloride / 2% v/v concentrated HCl solution was used as a reducing agent.

Samples from the labile Fe(II) extraction from the Claff extraction was measured after ca. 20 min, without addition of the hydroxyl-ammonium-chloride reducing agent. After the measurements of these extracts, they were measured again ca. 1 h after addition of the reducing agent, to determine the total labile Fe content. The difference between total labile Fe and labile Fe(II) represents the labile Fe(III) concentration. All other samples where measured after ca. 1 h.

3. Results

3.1. Porewater content

Figure 2 shows the porewater profiles of HS^-, Fe^{2+}, S, CH_4, P and NH_4^+ for both cores. The porewater profiles of S and P are similar to the SO_4^{2-} and PO_4^{3-} profiles (not shown), but were

analyzed at higher resolution. The HS^- profiles of PHOX 4 and PHOX 12 showed a rapid increase with depth to maxima of 1964 μM at a depth of 183 cm and 790 μM at a depth of 125 cm, respectively, although the PHOX 4 profile does show a minimum at 83 cm, in Unit II. This initial increase is followed by a gradual decrease to ca. 0 μM at 293 cm (PHOX 4) and 205 cm (PHOX 12), slightly above the sulfidization front (S.F.). Fe^{2+} concentrations remain ca. 0 μM until the S.F. at 293 cm (PHOX 4) and 205 cm (PHOX 12). Below The S.F. Fe^{2+} concentrations increase to ca. 700 μM in PHOX 4 and to ca. 400 μM in PHOX 12, with a peak at 780 cm of 780 μM. CH_4 concentrations start increasing at a depth of ca. 200 cm in both cores and reach concentrations of ca. 500 μM (PHOX 4) and ca.250 μM (PHOX 12).

At PHOX 4 the S profile showed a minimum at 83 cm. Otherwise the profile showed a downward diffusion trend, as well as, the influence of SO_4^{2-} reduction through the slight curvature of the profile, until values reach 0 μM at ca. 233 cm. The P profile showed an increase, from ca. 25 μM at 43 cm to ca. 200 μM at 283 cm, directly above the S.F. This is followed by a rapid decrease to 30 μM in the deepest part of the core. At PHOX 12 the porewater S profile shows a trend similar to PHOX 4 indicating downward diffusion and SO_4^{2-} reduction over the first 200 cm. Below 200 cm, S concentrations decrease at a less steep slope until it reaches a concentration of 0 μM at ca 800 cm, via downward diffusion only. The P profile showed a gradually increase to a maximum of ca. 35 μM at 200 cm, after which it decreases rapidly with ca. 20 μM.

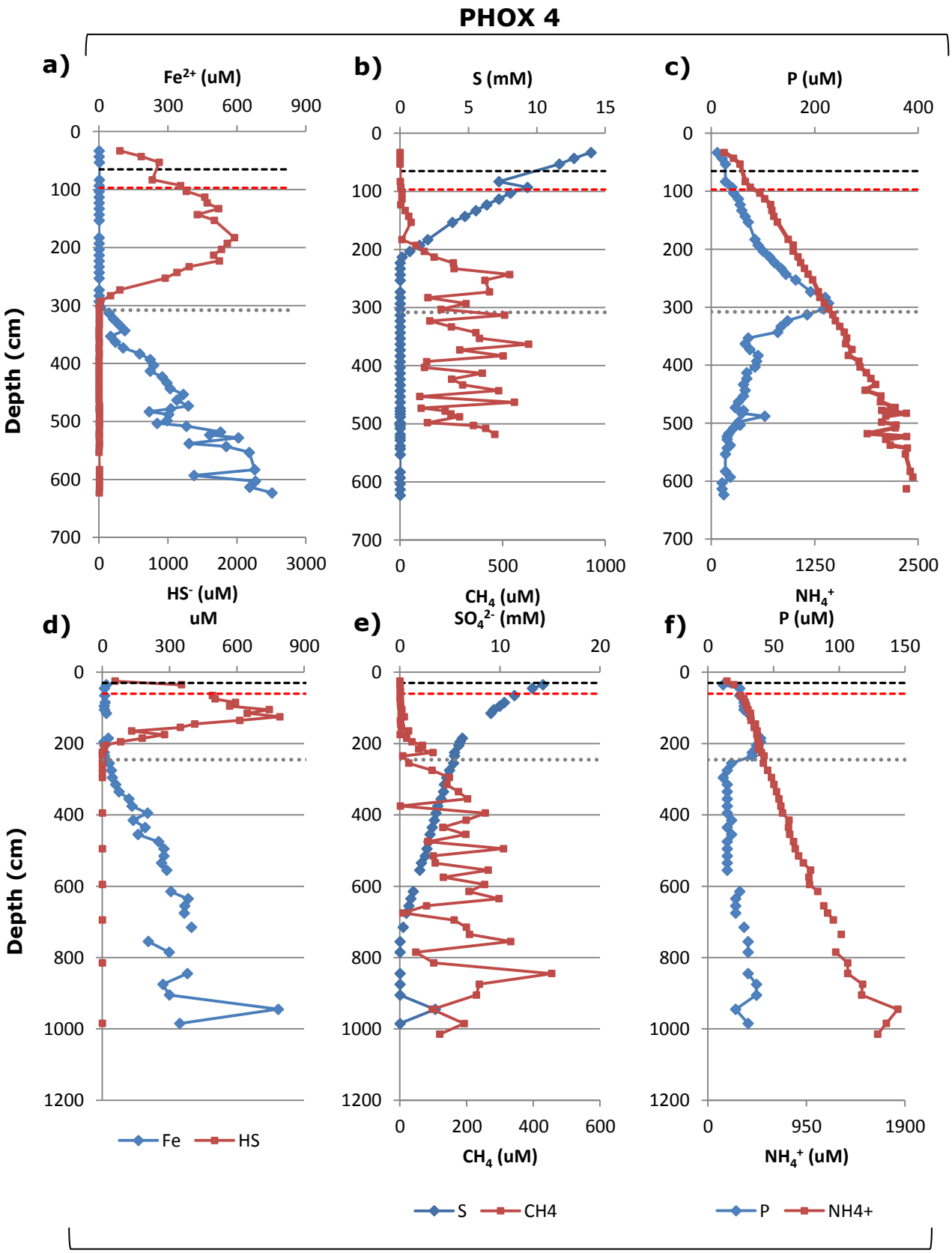

Figure 2. Porewater profiles of HS^-, Fe^{2+}, S^-, CH_4, P and NH_4^+ for PHOX 4(a, b, c) and PHOX 12 (d, e, f). The black dashed line indicates the Unit I/II transition, the red dashed line indicates the Unit II/III transition (i.e. the lake-marine transition) and the grey dotted line indicates the sulfidization front.

3.2. Solid phase content

3.2.1. Organic carbon

The Org. C profiles for both cores show the same general trend with a large initial increase, from ca. 4 wt-% in the marine sediments (Unit I) to ca. 14 wt-% (PHOX 4) and ca. 20 wt-% (PHOX 12) in the sapropel layer (Unit II). This is followed by a rapid decrease to ca. 0.5 wt-% (Fig. 3) in the lake sediments (Unit III). (Cruise report 2013) In PHOX 4 a smaller peak exist above Unit II at 65 cm, whereas in PHOX 12 a smaller peak can be seen below Unit II, at 95 cm.

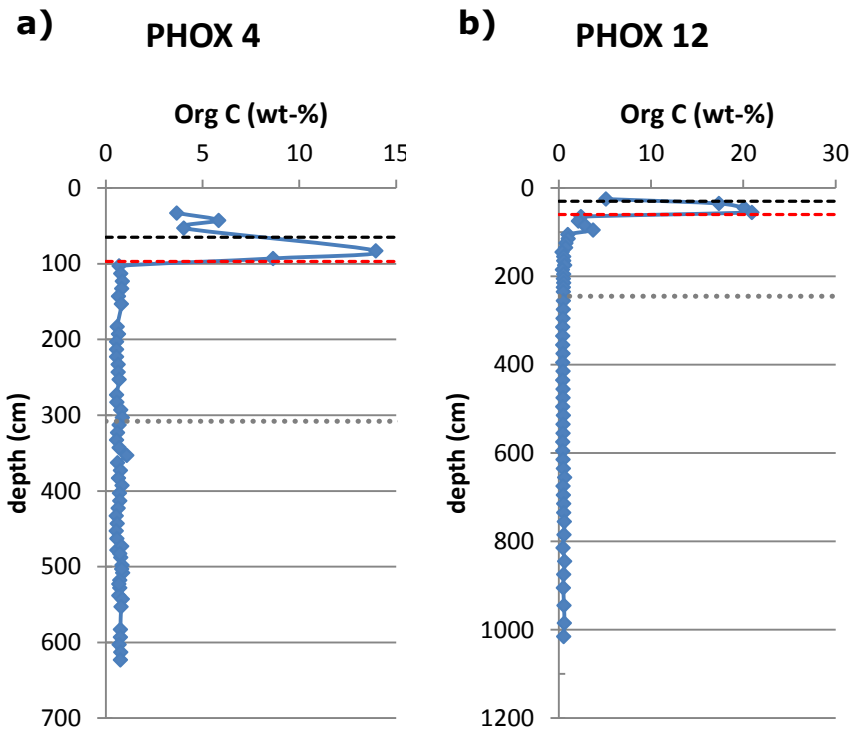

Figure 3. Org. C profile for PHOX 4 (a) and PHOX 12 (b). The black dashed line indicates the Unit I/II transition, the red dashed line indicates the Unit II/III transition (i.e. the lake-marine transition) and the grey dotted line indicates the location of the sulfidization front. Note that the scale of the vertical axis differs for PHOX 4 and PHOX 12.

3.2.2. Bulk solid phase constituents

Figure 4 shows the Al-normalized profiles for solid phase Fe, S, and P for both PHOX 4 and PHOX 12. All three elements show peaks coinciding with the Org. C peaks. Apart from this, the Fe profile remained relatively constant, whereas the S profile showed a continual decrease to values near 0 at depths of 313 cm (PHOX 4) and 255 cm (PHOX 12), defined as the S.F. At the same depths the P profile showed minor increases to a higher relatively constant level, except for distinct peaks at 363 cm (PHOX 4) and 395 cm (PHOX 12). Furthermore the P profile of PHOX 12 shows large increase at 1015 cm, which is most likely the result of contamination due to the coring process.

3.2.3. Iron speciation

The concentration profiles of the different Fe pools as identified by the Claff and Poulton extractions are shown in Fig. 5 (PHOX 4) and Fig. 6 (PHOX 12). In both cores, the profiles for labile Fe(II) (Fig. 5a, Fig. 6a) and Fe(III) (Fig. 5b, Fig. 6b) and for Carb. Fe (Fig.5e, Fig. 6e) showed similar trends with relatively low and even near 0 μmol/g (labile Fe(III) and Carb. Fe) concentrations over the first 240 cm (PHOX 4) and 185 cm (PHOX 12). Below these depths the concentrations rapidly

increased to ca. 150 μmol/g (PHOX 4) and ca. 225 μmol/g (PHOX 12) for Fe(II) and Carb. Fe, directly above the S.F.. The Fe(III) concentration increased to ca. 75 μmol/g and ca. 65 μmol/g, for PHOX 4 and PHOX 12 respectively. After this initial increase concentrations of all three pools remained high.

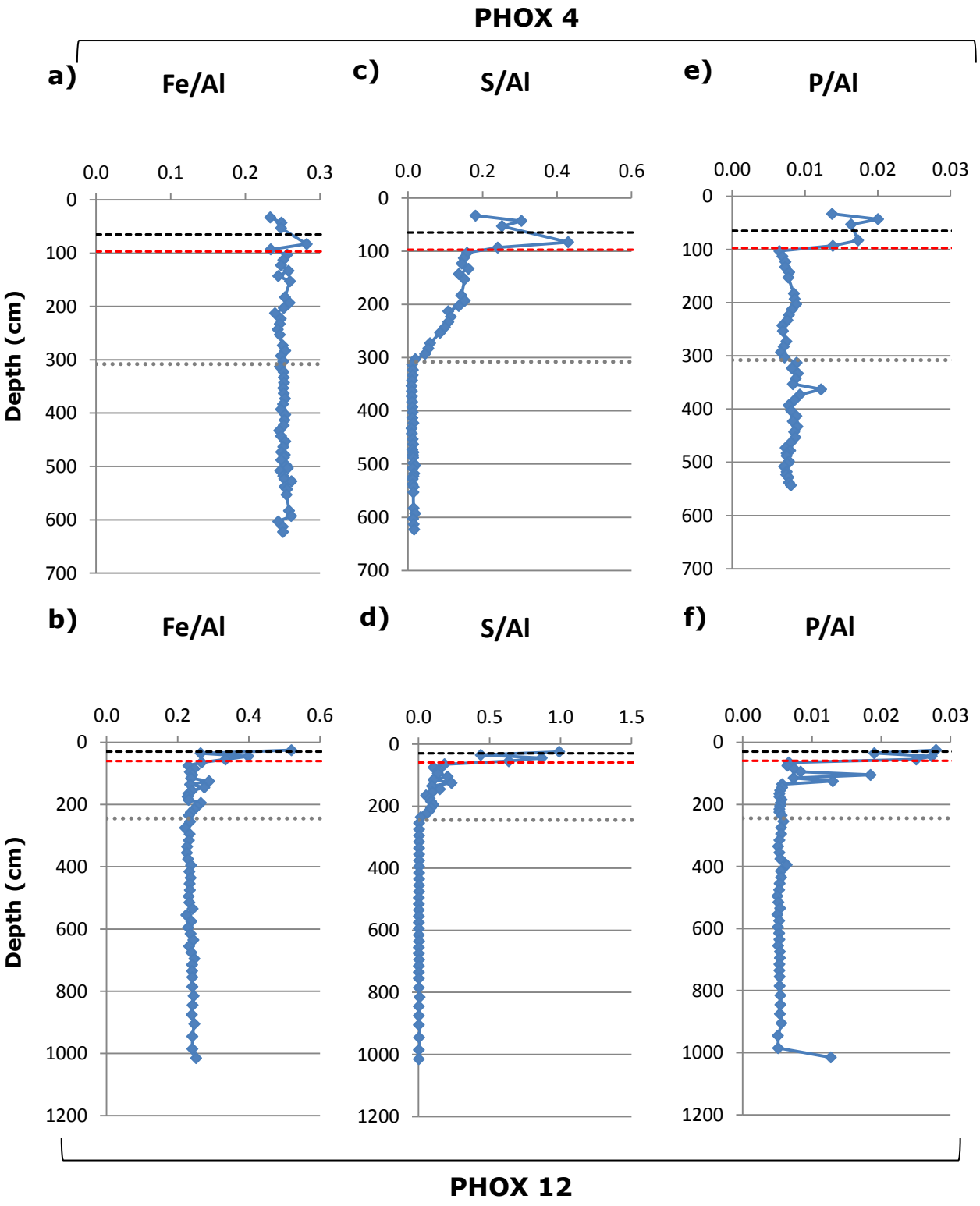

Figure 4. Al-normalized Fe, S and P content for both PHOX 4 (a, c, e) and PHOX 12 (b, d,f). The black dashed line indicates the Unit I/II transition, the red dashed line indicates the Unit II/III transition (i.e. the lake-marine transition) and the grey dotted line indicates the sulfidization front.

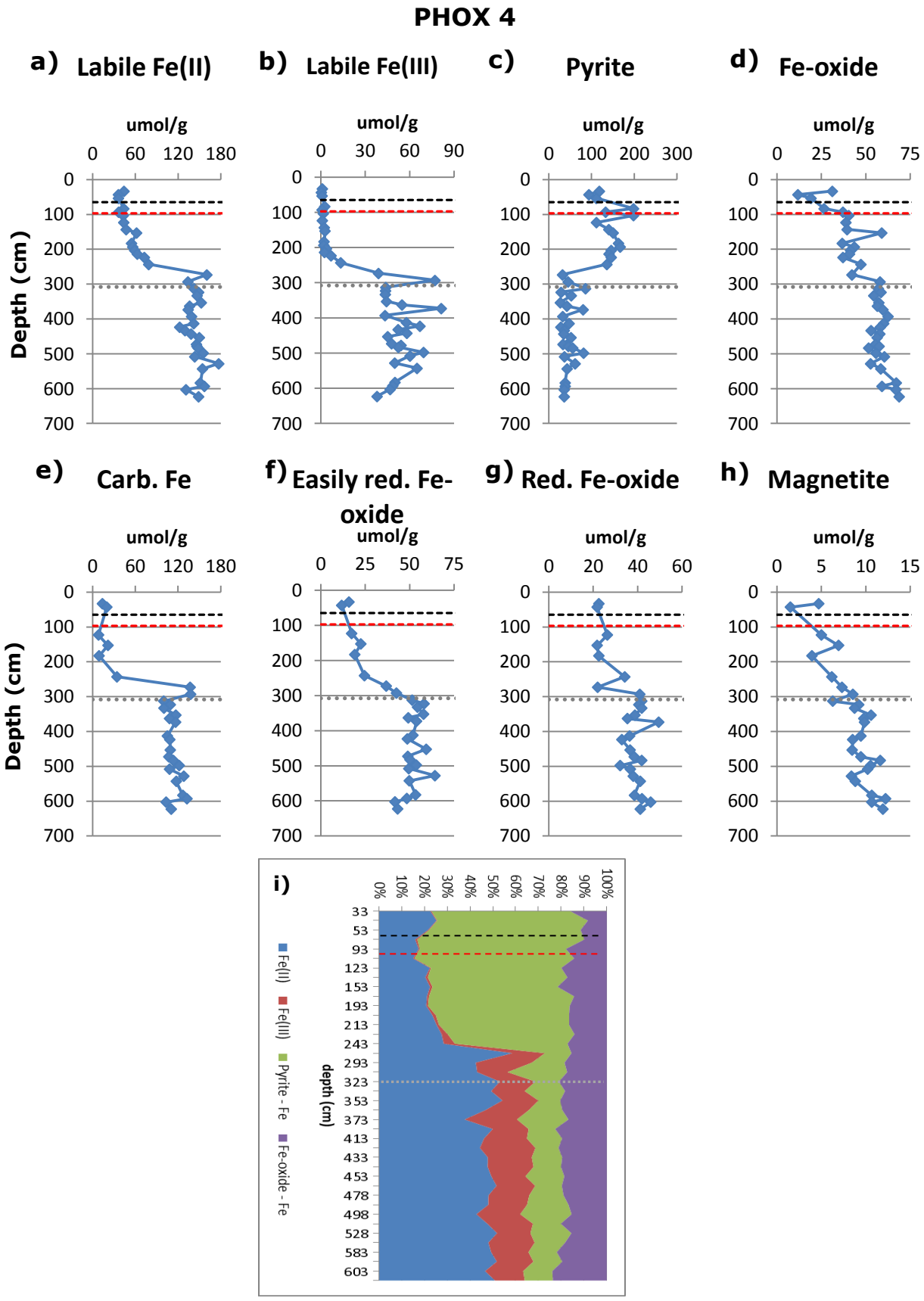

Figure 5. Iron speciation for PHOX 4. a – d) are results from the Claff extraction (Claff et al, 2010). e – h) are results from the Poulton extraction (Poulton and Canfield, 2005). (d) are all Fe-oxides, except for the labile Fe(III), which is shown in b). (f) easily reducible oxides, including ferrihydrite. (g) reducible oxides, including goethite and hematite. i) shows a cumulative plot of the pools from the Claff extraction.
The black dashed line indicates the unit I/II transition, the red dashed line indicates the unit II/III transition (i.e. the lake-marine transition) and the grey dotted line indicates the sulfidization front.

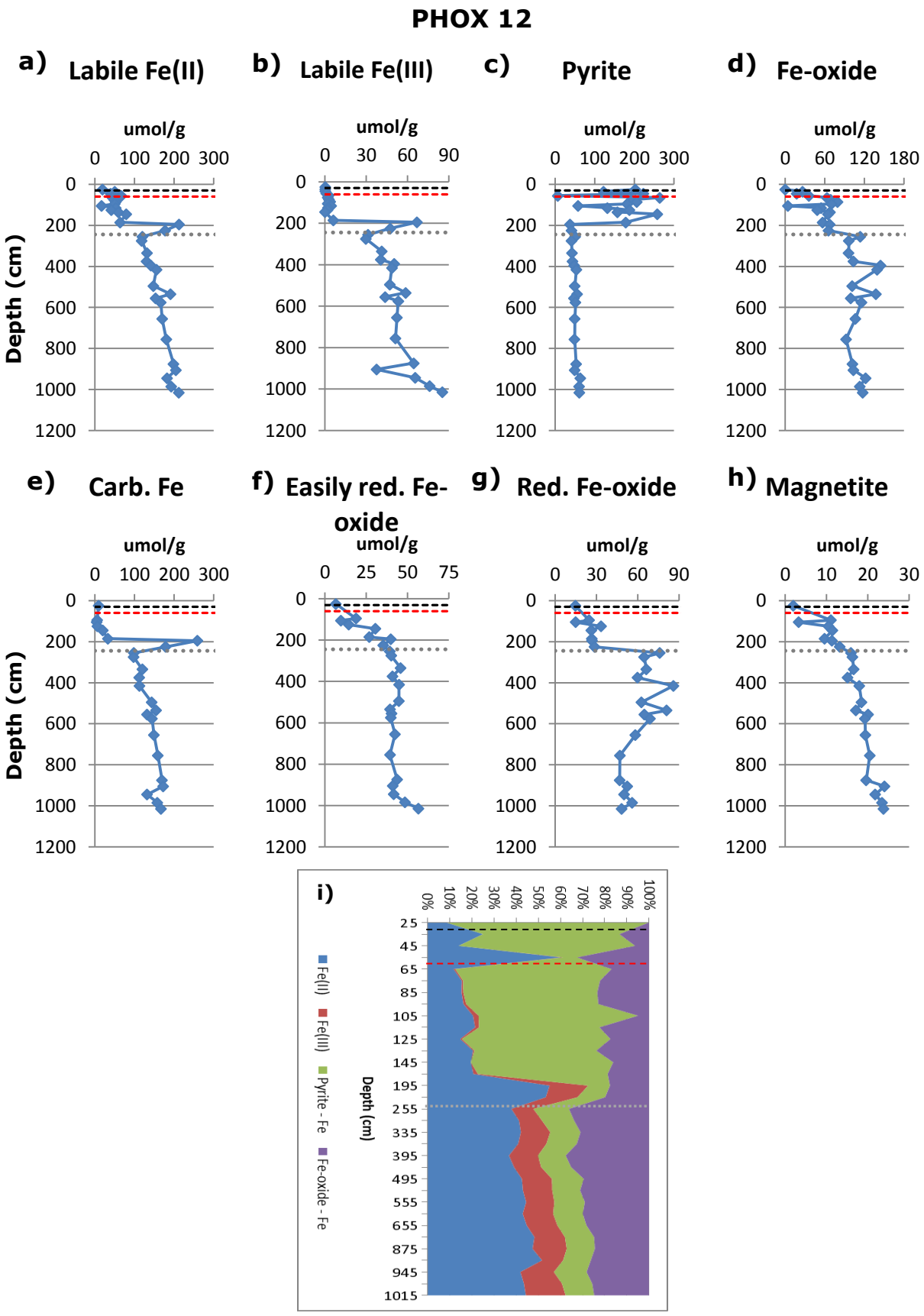

Figure 6. Iron speciation for PHOX 12. a – d) are results from the Claff extraction (Claff et al, 2010). e – h) are results from the Poulton extraction (Poulton and Canfield, 2005). (d) are all Fe-oxides, except for the labile Fe(III), which is shown in b). (f) easily reducible oxides, including ferrihydrite. (g) reducible oxides, including goethite and hematite. i) shows a cumulative plot of the pools from the Claff extraction.
The black dashed line indicates the unit I/II transition, the red dashed line indicates the unit II/III transition (i.e. the lake-marine transition) and the grey dotted line indicates the sulfidization front.

Magnetite concentrations (Fig. 5g, Fig. 6h) increased with depth in both cores, but remained low, with maxima of ca. 10 μmol/g (PHOX 4) and ca. 20 μmol/g (PHOX 12), at the most contributing no more than 10% to the total Fe pool (Fig. 5i, Fig. 6i). The other Fe oxide pools (crystalline Fe oxide [Claff] and easily red. Fe oxide and red. Fe oxide [Poulton]) showed an increase similar to, though less pronounced than, the Fe(II), Fe(III) and carbonate profiles at 240 cm(PHOX 4) and 185 cm (PHOX 12). This increase is best visible in the easily red. Fe oxide pool. The crystalline Fe oxide profile showed an extra similar increase at ca. 93 cm (PHOX 4) and ca. 60 cm (PHOX 12), which coincides with the lake-marine transition (cruise report 2013).

The pyrite profiles (Fig. 5c, Fig. 6c) showed an opposite trend, with high concentrations, up to ca 200 μmol/g (PHOX 4) and ca. 250 μmol/g (PHOX 12), in the top 240 cm (PHOX 4) and 185 cm (PHOX 12) of the sediments and low concentrations (ca. 30 μmol/g at PHOX 4 and ca. 40 μmol/g at PHOX 12) below the S.F. In the top of the sediments of both cores, pyrite contributes up to 70% to the total Fe pool, whereas in the deeper sediments it contributes ca. 10% (Fig. 5i, Fig. 6i).

3.2.4. Phosphorus speciation

The results of the SEDEX extractions are shown in Fig. 7 (PHOX 4) and Fig. 8 (PHOX 12). The Org. P profiles (Fig. 7a, Fig. 8a) have a maximum of ca. 12 μmol/g (PHOX 4) and of ca. 19 μmol/g (PHOX 12), in Unit II. After these peaks the concentration quickly drops to ca. 1 μmol/g in Unit III. PHOX 12 does have a minor secondary peak of ca. 8 μmol/g at 85 cm, directly below the lake-marine transition.

At PHOX 4, the Fe-bound P profile (Fig. 7b) showed relatively high concentrations (ca. 7 μmol/g) in Unit 1, dropping to ca. 2 μmol/g in Unit II. A smaller peak (ca. 4 μmol/g) is present at 183 cm in Unit III. The highest concentration of Fe-bound P is at a depth of 363 cm (ca. 14 μmol/g), below the S.F. Ca-bound P concentrations (Fig. 7c) increase from ca. 5 μmol/g in Unit I, to ca. 8 μmol/g in Unit II, after which it drops to ca. 3.5 μmol/g in Unit III. the Det. P (Fig. 7d) increases from ca. 2.5 μmol/g (Unit I/II) to ca. 4 μmol/g at the lake-marine transition, and ca. 7.5 μmol/g in Unit III. The exchangeable P profile (Fig. 7e) has maxima at 53 cm (Unit I/II transition) and 183 cm, but concentrations remain low resulting in a contribution to the total P pool of 1-2% on average (Fig. 7f).

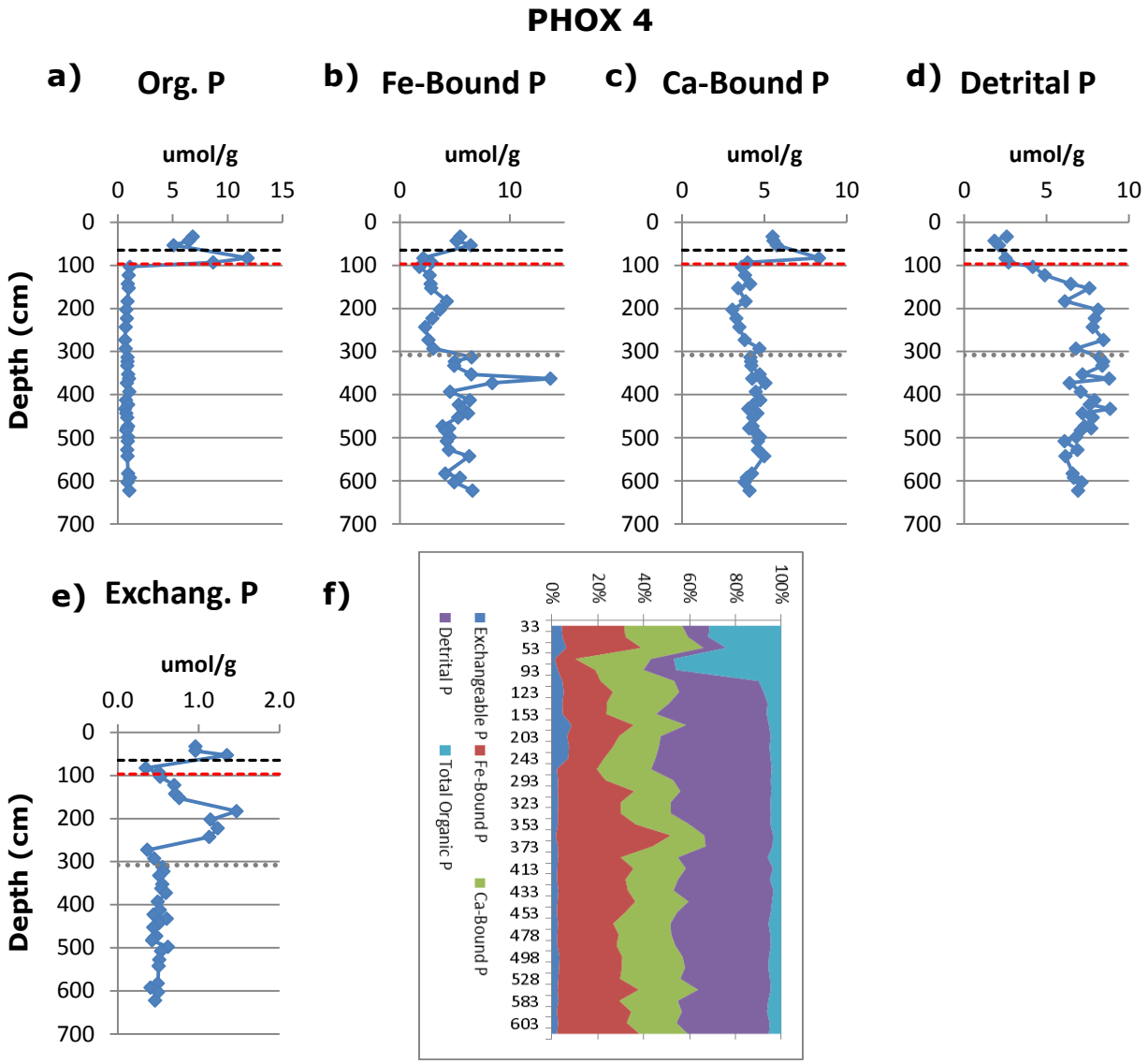

Figure 7. PHOX 4 P speciation (SEDEX; Ruttenberg, 1992). f) shows a cumulative plot of the pools. The black dashed line indicates the unit I/II transition, the red dashed line indicates the unit II/III transition (i.e. the lake-marine transition) and the grey dotted line indicates the sulfidization front.

The Fe-bound P profile at PHOX 12 (Fig. 8b) has maxima at 25 cm (ca. 6.4 μmol/g), 125 cm (ca. 5.7 μmol/g), 395 cm (7.2 μmol/g) and 1015 cm. This last peak is most likely a consequence of contamination due to the coring procedure. For most of the core concentrations are ca. 3.5-4 μmol/g. Ca-bound P concentrations (Fig. 8c) are ca. 6 μmol/g for most of the core, with maxima at 145 cm (ca. 11 μmol/g) and 1015 cm and a minimum of 3.4 μmol/g at 415 cm. The Det. P profile (Fig. 8d) shows a general increase throughout the core, from ca. 1.4 μmol/g at 25 cm to ca. 4.5 μmol/g at 985 cm. Between 65 cm and 135 cm, however, Det. P concentrations reach a maximum of ca. 4.7 μmol/g. Furthermore, a maximum concentration at 415 cm of ca. 7 μmol/g coincides with the minimum in Ca-bound P. Exchangeable P concentrations (Fig. 8e) remain low throughout the core, with an average contribution to the total P pool of ca 5% (Fig. 8f).

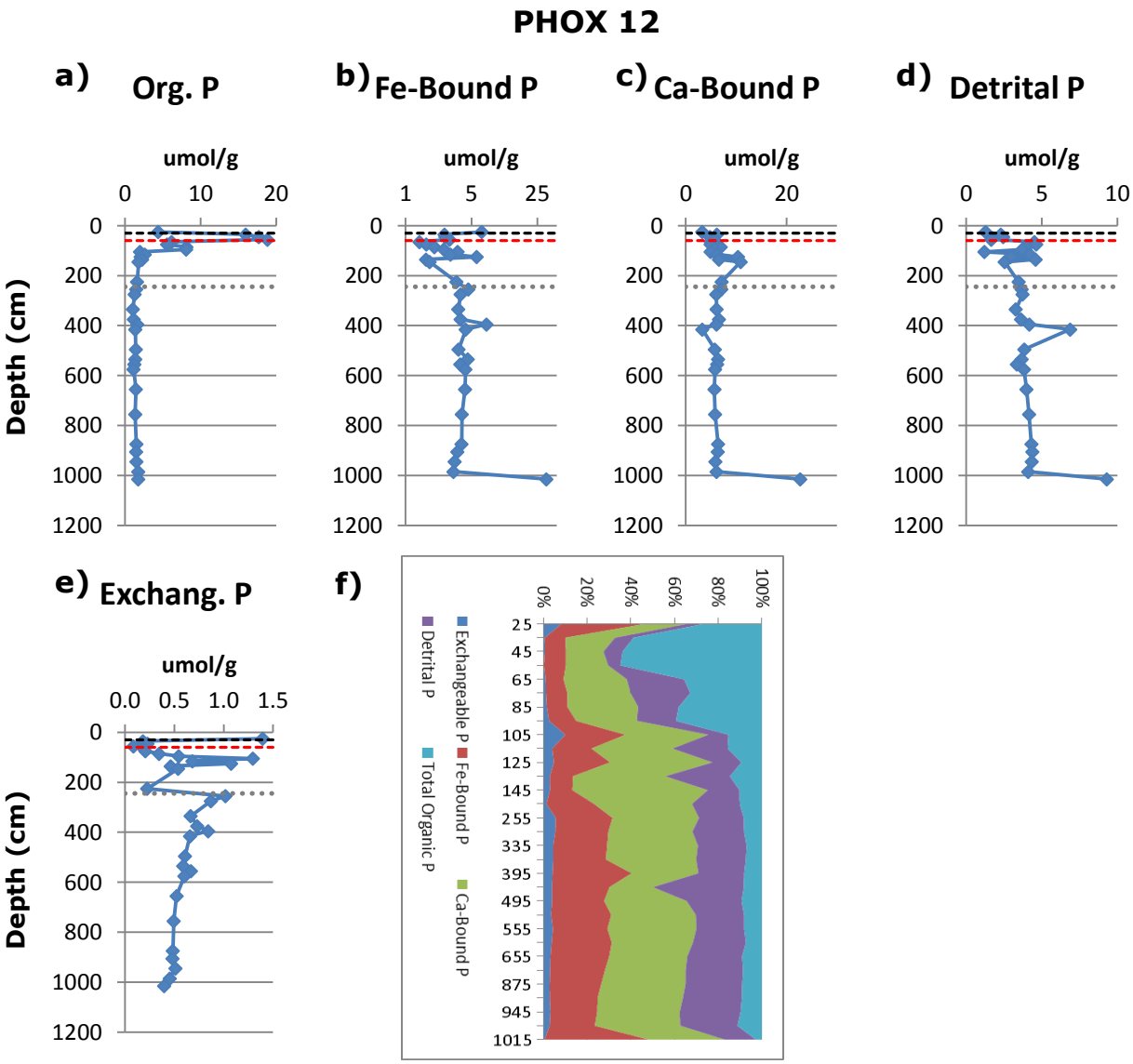

Figure 8. PHOX 12 P speciation (SEDEX; Ruttenberg, 1992). f) shows a cumulative plot of the pools. Note that the concentration of Fe-bound P is plotted on a logarithmic scale, with a base of 5. This is done to prevent the peak at 1015 cm to repress the signals of the rest of the core. The black dashed line indicates the unit I/II transition, the red dashed line indicates the unit II/III transition (i.e. the lake-marine transition) and the grey dotted line indicates the sulfidization front.

4. Discussion

4.1. Accumulation and preservation of iron and phosphorus in the surface sediments

Despite the strongly reducing conditions of the marine Black Sea bottom waters, the surface sediments (Unit I) at both PHOX 12 (<30 cm) and to a lesser extent PHOX 4 (< 60 cm) contain increased amounts of Al-normalized iron and phosphorus (Fig. 4). These increases in relative concentration can be explained by two main processes.

First, there is the transition from lacustrine to marine conditions, caused by the inflow of saline water from the Mediterranean through the Bosporus Strait into the Black Sea. This change in

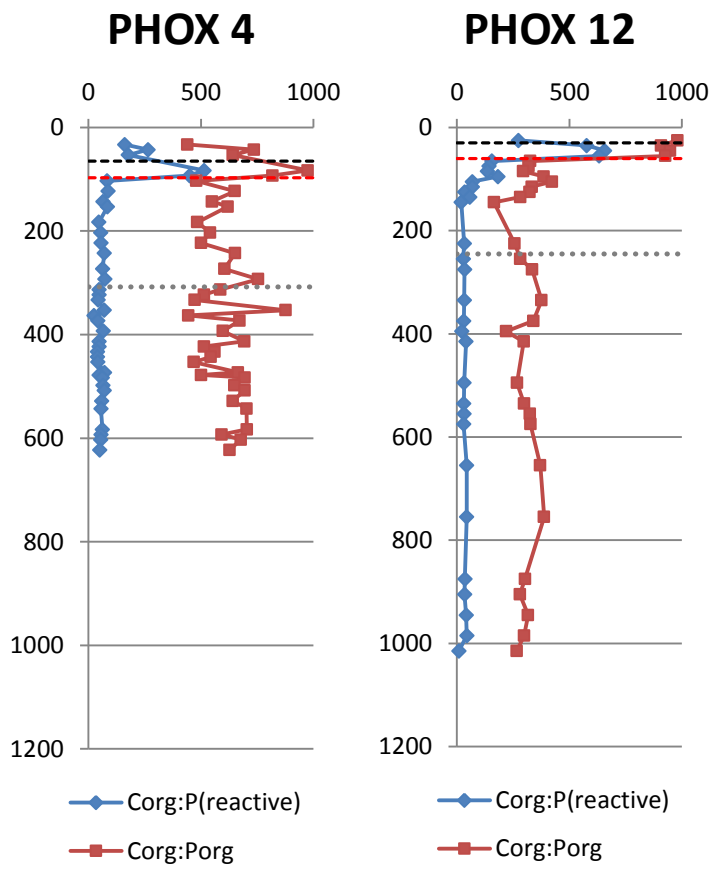

Figure 9. C_{org}:P(reactive) and C_{org}:P_{org} profiles for both PHOX 4and PHOX 12. Note the large change in both ratios at the lake-marine transition. The black dashed line indicates the unit I/II transition, the red dashed line indicates the unit II/III transition (i.e. the lake-marine transition) and the grey dotted line indicates the sulfidization front.

depositional environment, signifies a decrease in relative importance of the terrestrial input into the system under marine conditions, as is further evidenced in PHOX 4 by the changes in size of the sedimentary Ca-bound P and det P pools at the lake-marine transition (ca. 97 cm) (Fig. 7). As Det P is assumed to remain unaltered during deposition, its high concentration in the lacustrine sediment is an indication of the relative importance of terrestrial sources in this environment. Ca-bound P, on the other hand, is indicative of the relative importance of marine input. The decrease of the relatively aluminum rich terrestrial input into the system, consequently, contributes to the increasing Al-normalized iron and phosphorus concentrations, due to the decreased input of aluminum.

Furthermore, the lake-marine (ca. 97 cm at PHOX 4; ca. 60 cm at PHOX 12) transition also accounts for the relatively high Org P concentrations in Units I and II at both sites (Fig. 9). Under the euxinic conditions of the marine Black Sea OM is better preserved, than under the oxic conditions of the Lacustrine Black Sea. Despite the increased recycling efficiency of Org P under anoxic conditions (Fig. 9) (Arthur and Dean 1998, Slomp et al 2002), the increased preservation of OM still results in an increased preservation of Org P in the marine environment, compared to the lacustrine environment.

The second process that can be an important contributor to the increased concentrations of the normalized iron and phosphorus in the surface sediment is an active iron shuttle. By transporting Fe (oxyhydr)oxides from the shelf, via the slope and into the deep basin (Fig. 10), the concentration of iron on the slopes and primarily in the deep basin increases, resulting in higher concentrations of iron in the surface sediments, despite strongly reducing conditions ((Lyons And

Severmann 2006; Wijsman et al 2001, Scholz et al 2014). By adsorption or co-precipitation of phosphorus to these Fe (oxyhydr)oxides transported down from the shelf, The Fe-bound P pool can be increased as well (Shaffer 1986; Dellwig et al 2010).

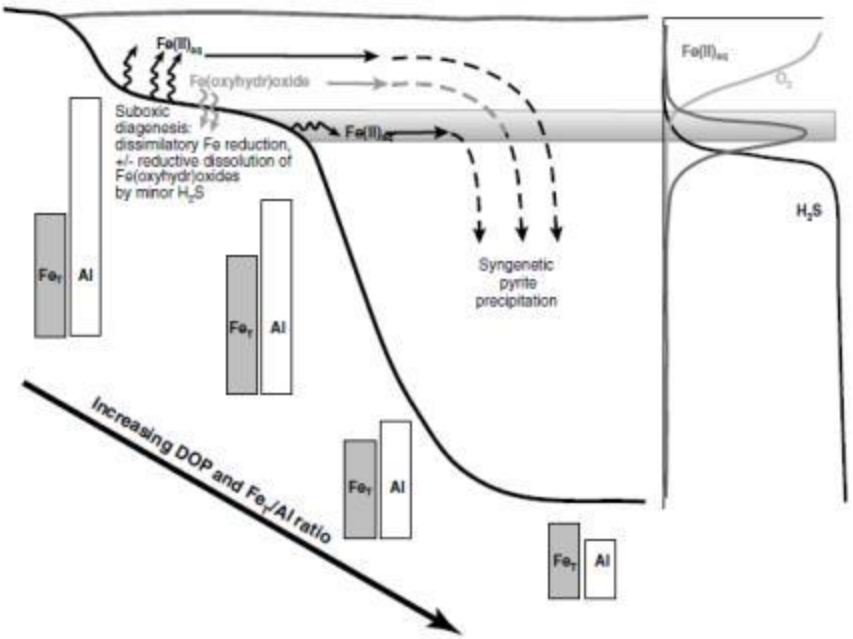

Figure 10. Schematic representation of the Fe shuttle (Lyons and Severmann 2006).

This theory, of an active iron shuttle as an important input of iron and phosphorus, is in concordance with the relatively high concentrations of Fe oxide and Fe-bound P at PHOX 4 (Fig. 11). However, at PHOX 12 Fe oxide concentrations in the surface sediments are low, despite the increase in Fe/Al. This can be explained by the complete reduction of the transported Fe oxides, due to the reaction with HS^-, as Dellwig et al (2010) already proposed for the strongly euxinic Black Sea. As a result, Fe oxides transported into the deep basin from the shelf is deposited as FeS_2 instead. Consequently, the iron shuttle cannot account for the increased Fe-bound P concentration in the surface sediment of PHOX 12.

Possibly, this increase in Fe-bound P is the result of upward diffusion of PO_4^{3-} (Fig. 11) released from the Unit II sapropel, as a result of the decomposition of the OM from the sapropel, into the surface sediments (Unit I). There it might subsequently react with Fe^{2+} in the porewater, increasing the Fe-P pool. This, however, assumes that HS^- concentrations in the porewater are low enough not to outcompete the PO_4^{3-}. As Fig. 11 shows, HS^- concentrations in the surface sediment of PHOX 12 are in indeed relatively low, which would support the theory of a reaction between PO_4^{3-} and Fe^{2+} in the porewater. Nonetheless, HS^- concentrations (ca. 60 µM) seem to remain high enough to scavenge all Fe^{2+} from the porewater.

4.2. Phosphorus accumulation below the sulfidization front.

Aside from the lake-marine transition, which changed the depositional environment resulting in changes in the iron and phosphorus pools, the sediment from the Black Sea is also influenced by diagenetic overprinting as a consequence of the infiltration of SO_4^{2-} into the lake sediment, its reduction to HS^- and the subsequent reaction between HS^- and Fe (oxyhydr)oxides in the sediment. This results in the existence of a sulfidization front, recognizable in the sediments of both PHOX 4 (ca. 308 cm) and PHOX 12 (ca. 245 cm).

Above the sulfidization front, Fe oxides deposited under lacustrine conditions have been largely reduced through reaction with the HS^- in the porewater, resulting in the formation of the FeS and FeS_2. Relatively high concentrations of FeS, formed as an intermediary step in the formation of FeS_2, are likely present directly above the sulfidization front (Holmkvist et al 2004;Jørgensen et al 2004). The maxima in carb-Fe and labile Fe(III) (Fig. 5, Fig. 6) located directly above the sulfidization front likely represent erroneously identified FeS, resulting in expected FeS concentrations of ca. 90 µmol/g (PHOX 4) and ca. 240 µmol/g (PHOX 12).

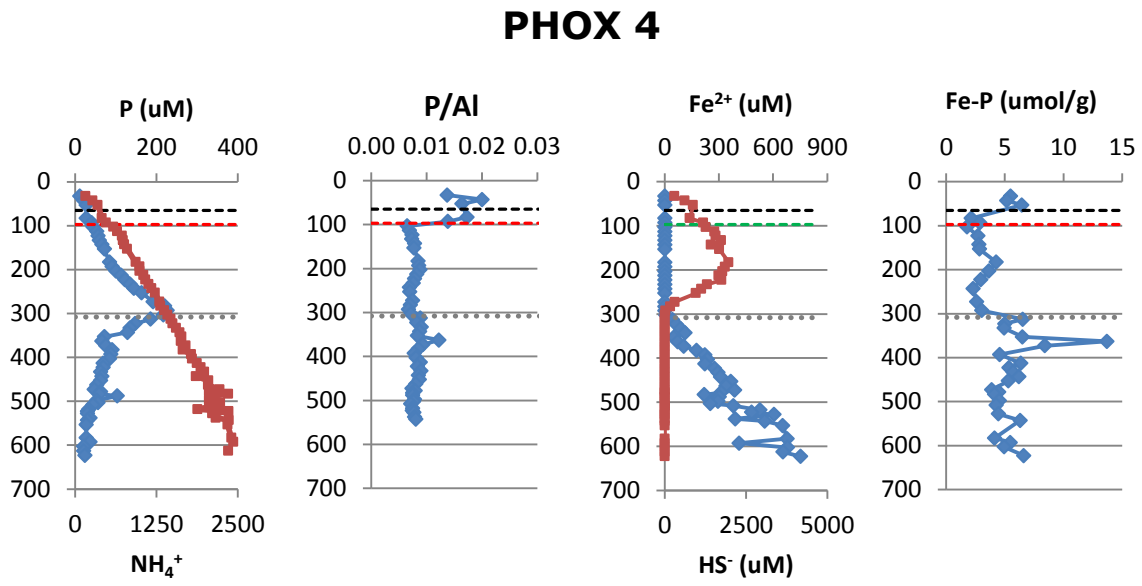

Figure 11. Porewater profiles of P, NH_4^+, Fe^{2+} and HS^-, as well as solid phase profiles of P/Al amd Fe-P for PHOX 4. Note how Fe-bound P and P/Al have maxima at 363 cm, and PO_4^{3-} amd Fe^{2+} have minma at the same depth. The black dashed line indicates the unit I/II transition, the red dashed line indicates the unit II/III transition (i.e. the lake-marine transition) and the grey dotted line indicates the sulfidization front.

Similar values (ca. 80 µmol/g for PHOX 4 and ca. 260 µmol/g for PHOX 12) can be obtained based on the total sedimentary Sulphur and pyrite data, indicating that these maxima in labile Fe(III) and carb-Fe are indeed related to FeS.

Besides forming FeS and FeS_2, the reaction between Fe oxides and HS^- also results in the release of phosphorous bound to these Fe oxides to the porewater in the form of PO_4^{3-} (Fig. 11). This PO_4^{3-} subsequently diffuses both up and down into the sediment. The downward diffusing PO_4^{3-} can come into contact with Fe^{2+} (Fig. 11) present in the porewater below the sulfidization front and, as a result, form Fe-P minerals such as vivianite. This explains the coinciding peaks in P/Al and Fe-bound P at ca. 363 cm PHOX 4, as well as, the less pronounced, peaks at ca. 400cm in PHOX 12 (Fig. 11), both well below the sulfidization front.

The accumulation of phosphorus below the sulfidization front also provide a potential explanation for the minor peaks in P/Al and Fe-bound P at ca. 190 cm (PHOX 4) and ca. 125 cm (PHOX 12). If a similar downward diffusion and accumulation of phosphorus occurred with a higher sulfidization front, possibly at the lake-marine transition, peaks similar to those found at ca. 363 cm (PHOX 4) and ca. 400 cm (PHOX 12) would have formed. As a result of a subsequent deeper infiltration of HS^- and, therefore, a downward movement of the sulfidization front, the peaks formed below to old sulfidization front will be overprint and largely lost, via the reaction of the iron minerals with the HS^-. The aforementioned peaks at ca. 190 cm (PHOX 4) and ca. 125 cm (PHOX 12) might be remnants of such accumulation features.

4.2.1. Possible Influence of AOM

In addition to the diagenetic overprint of the lacustrine deposits by the sulfidization of iron, the sediments in the Black Sea might also be influenced by AOM. Most often AOM is a reaction between CH_4 and SO_4^{2-} resulting in the formation of HS^-. Recent studies (e.g. Beal et al 2009; Egger et al 2015), however, propose alternative pathways by which AOM can take place in the absence of SO_4^{2-}. A possible alternative is the reaction between Fe (oxyhydr)oxides and CH_4 (Eq 2). The HCO_3^- formed as a result can react with the Fe^{2+} to form carb-Fe. This can explain the relatively high concentrations of carb-Fe below the sulfidization front at both sites.

Furthermore the strange behavior of SO_4^{2-} at PHOX 12 seems to be correlated to the presence of CH_4, as the onset of CH_4 in the porewater coincides with the change in diffusion speed in SO_4^{2-}.

4.3. Spatial differences and similarities in the Black Sea

Aside from temporal changes to the sediment record, there are also distinct spatial differences in the sediment of the Black Sea. Comparison of the sites shows that the similar features caused by similar processes are present in the sediment of both sites. There is, however, a marked difference between the depths at which these features are evident. In the sediment of the deep basin (PHOX 12; 1969 mbss) the Unit I/II and Unit II/III transitions (i.e. the lake-marine transition),

as well as the sulfidization front is located at a shallower depth, than in the sediment of the slope site (PHOX 4; 377 mbss).

This difference in depth is likely a consequence of differences in sedimentation rates. A quick estimation of the sedimentation rates based on the unit thickness and the correlating time interval from literature (Eckert et al. 2013), results in an average sedimentation rate for Unit I and II of ca. 0.127 mm/yr. for PHOX 4, which is similar to the rates found by Roepert (2014). A similar estimation for PHOX 12 gives a value of ca. 0.079 mm/yr., approximately 1.6 times less than PHOX 4. The values of Both PHOX 4 and PHOX 12 are in close resemblance with the range given by Degens and Ross (1972) of 0-10 cm/ka, although the sedimentation rate at PHOX 4 is slightly high.

Consequently, as less material is being deposited in the deep basin than on the slope, less sediment can accumulate over the same time period. In other words, a given time period is represented in a smaller amount of sediment in the deep basin, compared to the slope. As such

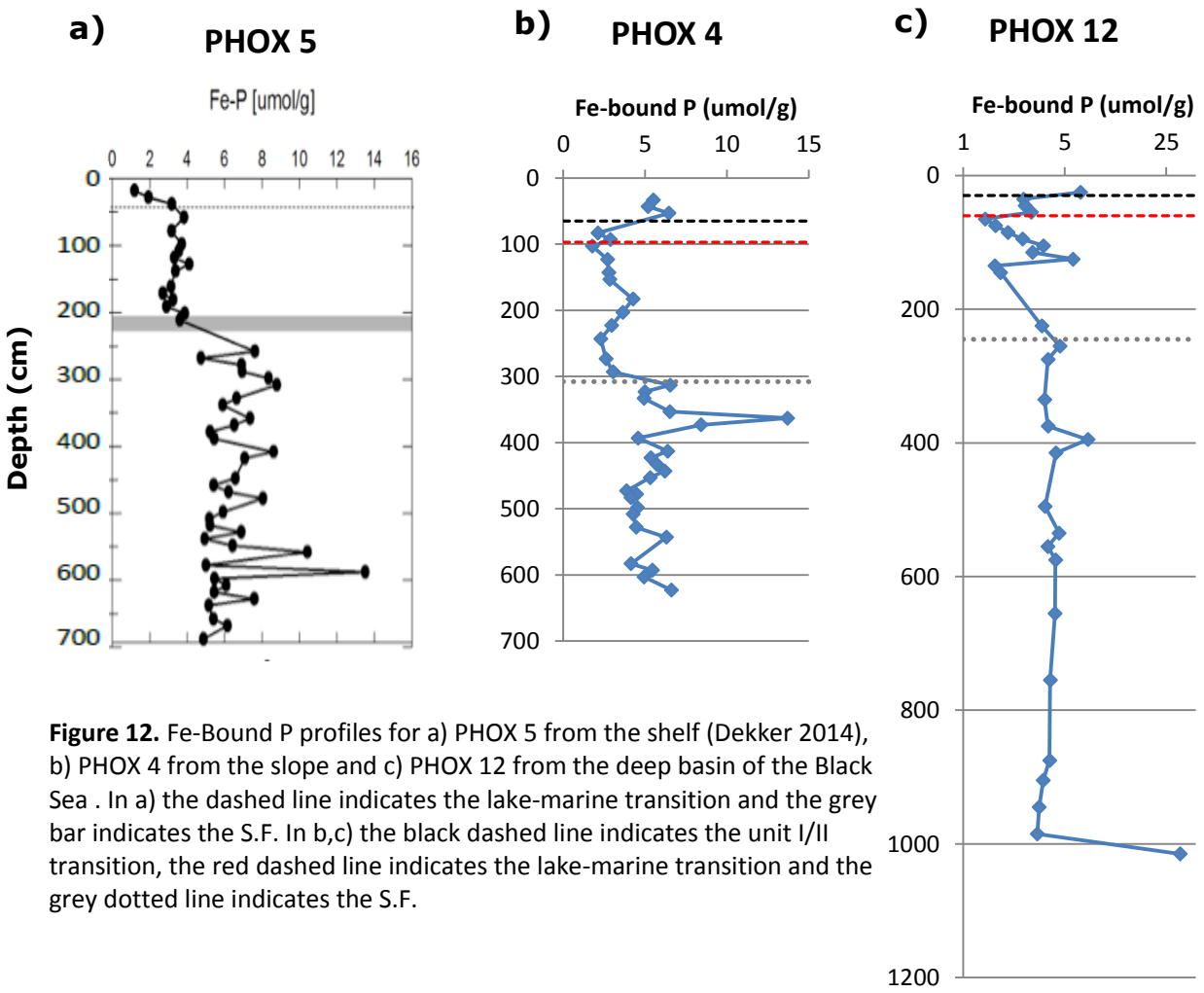

Figure 12. Fe-Bound P profiles for a) PHOX 5 from the shelf (Dekker 2014), b) PHOX 4 from the slope and c) PHOX 12 from the deep basin of the Black Sea . In a) the dashed line indicates the lake-marine transition and the grey bar indicates the S.F. In b,c) the black dashed line indicates the unit I/II transition, the red dashed line indicates the lake-marine transition and the grey dotted line indicates the S.F.

the depths at which the unit transitions are located within the sediment are shallower for PHOX 12 than for PHOX 4. Furthermore, assuming the movement of the sulfidization front takes place at roughly the same rate, it should be positioned at approximately the same depth below the lake-

marine transition. With a depth difference ca. 200 cm at PHOX 4 and ca. 185 cm at PHOX 12, this appears to be the case. As a consequence, the Sulfidization front is situated at a shallower depth in PHOX 12 as well.

Moreover, the influence of the lower sedimentation rate in PHOX 12 is also evident from the Al-normalized Fe profiles (Fig. 4a, b). The closer proximity of riverine outflows to PHOX 4 compared to PHOX 12 results in a larger input of Al-rich sediments from terrestrial origins.

As a consequence, the Al-normalized Fe profile of PHOX 4 shows a decrease at the top of the sediment. Contrarily, the Al-normalized Fe profile of PHOX 12 shows a marked increase in concentration, as there is less input of Al-rich sediments. Similarly, changes in terrestrial input due to the change from a lacustrine to a marine environment, which are clearly reflected in the PHOX 4 Ca-bound P and Det. P profiles, have a less pronounced effect on PHOX 12.

Aside from a difference in sedimentation rate, the sites are also influenced differently by the iron shuttle, as is exemplified by the Fe-bound P profiles (Fig. 12, 10). Including data from PHOX 5, a shelf site (178 mbss), it becomes evident that there is transport of iron and associated phosphorus from the shelf (PHOX 5; 178mbss) (Dekker 2014) with low concentrations of Fe-bound P, via the slope (PHOX 4; 377mbss) with higher concentrations, into the deep basin (PHOX 12; 1969 mbss) with still higher concentrations. As such, Fe oxide, originally deposited on the shallow shelf is remobilized and transported down the slope, were a small amount is deposited, into the deep basin of the Black Sea, were the Fe oxides accumulate.

5. Conclusions

With the onset of marine conditions ca. 9 ka the Fe and P geochemistry in the Black Sea changed significantly. While Fe oxides and Fe carbonates are major contributors to the total Fe pool under the oxic lacustrine condition, only the less reducible Fe oxides remain under the euxinic marine conditions. The other Fe carbonates and most of the Fe oxides react with the HS^- present in the marine environment and form FeS_2. The enrichment of iron in the surface sediment is primarily the result of two processes. The transition from lacustrine to marine conditions is in itself the source of a decrease in relative importance of terrestrial input, as is also evident from the change from det P (which is of terrestrial origin) to Ca-bound P (which indicates marine input) as an important sink for phosphorus in the sediment. This decrease in input of relatively Al-rich terrestrial matter consequently results in the increasing Al-normalized concentrations of Fe and P. The second important process is the active iron shuttle. By transporting Fe-oxides from the shelf into the deep basin the concentration of iron in the surface sediment of the basin increases. By

adsorption or co-precipitation of phosphorus to the Fe oxides phosphorus concentration in the surface sediment may increase, despite reducing conditions of the water column.

Concurrently, the infiltration of HS^- into the lacustrine sediments results in the diagenetic overprint of the lake sediments above the sulfidization front. Consequently lacustrine sediments above the sulfidization front are depleted in Fe-oxides. The reaction of these Fe-oxides with the HS^- directly above the sulfidization front results in the release of Fe-bound P into the porewater. Due to the downward diffusion of this phosphorus and the subsequent reaction with Fe^{2+} in the porewater, forming Fe-P minerals such as vivianite, an enrichment in Fe-bound P is formed below the sulfidization front. This same process may also explain minor peaks above the current sulfidization front as remnants of an older, shallower sulfidization front. This implies a phased downward movement of the sulfidization front.

An alternate potential source of diagenetic overprint is Fe-mediated AOM. The reaction between Fe oxides and CH_4 below the sulfidization front, may result in a decrease in Fe oxide concentrations. At the same time, the HCO_3^-, released during Fe-mediated AOM might react with the Fe^{2+} in the porewater, thereby forming Fe carbonates. This could explain the large concentration of Fe carbonates in the lacustrine sediments below the sulfidization front.

Placing the data in a spatial context shows that difference in sedimentation rates results in shallower depths at which different features (e.g. lake-marine transition and sulfidization front) are evident. The deeper the site is located the lower the sedimentation rate appears to be, resulting in shallower depth at which the different features are present in the sediment.

Furthermore, the relative importance of the iron shuttle becomes more apparent, as there is a clear trend of Fe and Fe-bound P concentrations increasing from the shelf (178 mbss), via the slope (377 mbss), into the basin (1969 mbss). However, since Fe oxide concentrations are very low in the deep basin, other processes seem to be active as well, allowing the accumulation and preservation of Fe-bound P in the surface sediments of the deep basin.

Acknowledgements

My thanks go to Peter Kraal and Caroline Slomp for their supervision, guidance and support for the duration of this project. Further thanks go to Tom Claessen, Dineke van de Meent and Natasja Welters for their help and patience in the use of the labs, as well as to Ton Zalm for the ICP-OES analyses and Arnold van Dijk for the CN analysis of my samples. Furthermore, my gratitude goes to all participants of the 2013 PHOXY cruise for the use of the samples and data and to all others who've supported me in the course of this project.

References

Arthur MA., Dean WE. 1998. Organic-matter production and preservation and evolution of anoxia in the Holocene Black Sea. Paleoceanography 13: 395-411

Bahr A., Lamy F., Arz HW., Kuhlmann H., Wefer G. 2005. Late glacial to Holocene climate and sedimentation history in the NW Black Sea. Marine Geology 214: 309-22.

Barnes RO. and Goldberg ED. 1976. Methane production and consumption in anoxic marine sediments. Geology 4: 297-300.

Beal EJ., House CH., Orphan VJ. 2009. Manganese- and iron-dependent marine methane oxidation. Science 325: 184-7.

Claff SR., Sullivan LA., Burton ED., Bush RT. 2010. A sequential extraction procedure for acid sulfate soils: Partitioning of iron. Geoderma 155: 224-30.

Cruise report PHOXY 2013, R/V Pelagia. 64PE371.

Degens ET., and Ross DA. 1972. Chronology of the Black Sea over the last 25,000 years. Chemical Geology 10: 1-16.

Dekker E. 2014 Influence of the lake/marine transition on phosphorus dynamics in Black Sea sediments below the redoxcline. BSc Thesis, Utrecht University.

Delaney ML. 1998. Phosphorus accumulation in marine sediemnts and the oceanic phosphorus cycle. Global Biogeochemical Cycles 12: 563-72.

Dellwig O., Leipe T., März C., Glockzin M., Pollehne F., Schnetger B., Yakushev EV., Böttcher ME., Brumsack H-J. 2010. A new particulate Mn-Fe-P shuttle at the redoxcline of anoxic basins. Geochimica et Cosmochimica Acta 74: 7100-15.

Diaz RJ., and Rosenberg R. 2008. Spreading Dead Zones and Consequences for Marine Ecosystems. Science, New Series 321: 926-9.

Dijkstra N., Kraal P., Kuypers MMM., Schnetger B., and Slomp CP. 2014. Are Iron-Phosphate Minerals a Sink for Phosphorus in Anoxic Black Sea sediments? PLoS One 9: e101139.

Eckert S., Brumsack H-J., Severmann S., Schnetger B., Märtz C., Henning Fröllje H. 2013. Establishment of euxinic conditions in the Holocene Black Sea. Geology 41: 431-4.

Egger M., Rasigraf O., Sapart CJ., Jilbert T., Jetten MSM., Röckmann T., Van der Veen C., Bânda N., Kartal B., ettwig KF., Slomp CP. 2015. Iron-Mediated Anaerobic Oxidation of Methane in Brackish Coastal Sediments. Environmental Science & Technology 49: 277-83.

Froelich PN., Arthur MA., Burnett WC., Deakin M., Hensley V., JahnkeR., Kaul L., Kim K-H., Roe K., Soutar A., Vathakanon C. 1988. Early diagenesis of organic matter in Peru continental margin sediments: Phosphorite precipitation. Marine Geology 80: 309-43.

Froelich PN., Bender ML., Heath GR. 1977. Phosphorus accumulation rates in metalliferous sediments on the East Pacific Rise. Earth and Planetary Science Letters 34: 351-9.

Froelich PN., Bender ML., Luedtke NA. 1982. The marine phosphurus cycle. American Journal of Science 282: 474-511.

Golterman HL. 1995. The role of the ironhydroxide-phosphate-sulphide system in the phosphate exchange between sediments and overlying water. Hydrobiologia 297: 43-54.

Holmkvist L., Kamyshny Jr A.., Vogt C., Vamvakopoulos K., Ferdelman TG., Jørgensen BB. 2011. Sulfate reduction below the sulfate–methane transition in Black Sea sediments . Deep-Sea Research I 58: 493-504.

Ingall ED., Bustin RM., Van Cappellen P. 1993. Influence of water column anoxia on the burial and preservation of carbon and phosphorus in marine shales. Geochimica et Cosmochimica Acta 57: 303-16.

Ingall ED. and Jahnke R. 1997. Influence of water-column anoxia on the elemental fractionation of carbon and phosphorus during sediment diagenesis. Marine Geology 139: 219-229.

Ingall ED., Kolowith L., Lyons T., Hurtgen M. 2005. Sediment carbon, nitrogen and phosphorus cycling in an anoxic fjord, Effingham Inlet, British Columbia. American Journal of Science 305: 240-58.

Jilbert T., and Slomp CP. 2013. Iron and manganese shuttles control the formation of authigenic phosphorus minerals in the euxinic basins of the Baltic Sea. Geochimica et Cosmochimica Acta 107: 155-69.

Jørgensen BB., Böttcher ME., Lüschen H., Neretin LN., Volkov II. 2004. „Anaerobic methane oxidation and a deep H2S sink generate isotopically heavy sulfides in Black Sea sediments." Geochimica et Cosmochimica Acta 68: 2095-118.

Kraal P., and Slomp CP. 2014. Rapid and Extensive Alteration of Phosphorus Speciation during Oxic Storage of Wet Sediment Samples. PLoS One 9: e96859.

Kraal P., Slomp CP., Forster A., Kuypers MMM., Sluijs A. 2009. Pyrite oxidation during sample storage determines phosphorus fractionation in carbonate-poor anoxic sediments. Geochimica et Cosmochimica Acta 73: 3277-90.

Kraal P., Slomp CP., Forster A., Kuypers MMM. 2010. Phosphorus cycling from the margin to abyssal depths in the proto-Atlantic during oceanic anoxic event 2. Palaeogeography, Palaeoclimatology, Palaeoecology 295: 42-54.

Kraal P., Slomp CP., Reed DC., Reichart G-J., Poulton SW. 2012."Sedimentary phosphorus and iron cycling in and below the oxygen minimum zone of the northern Arabian Sea. Biogeosciences 9: 2603-24.

Krom MD.,and Berner RA. 1981. The diagenesis of phosphorus in a nearshore marine sediment. Geochimica et Cosmochimica Acta 45: 207-16.

Krom MD., and Sholkovitz ER. 1978. On the association of iron and manganese with organic matter in anoxic marine porewaters. Geochimica et Cosmochimica Acta 42: 607-11.

Lyons TW. and Severmann S. 2006. A critical look at iron paleoredox proxies: New insights from modern euxinic marine basins. Geochimica et Cosmochimica Acta 70: 5698-722.

Meybeck M. 1982. Carbon, nitrogen and phosphorus transport by world rivers. American Journal of Science 282: 401-50.

Poulton SW. and Canfield DE. 2005. Development of a sequential extraction procedure for iron: implications for iron partitioning in continentally derived particulates. Chemical Geology 214: 209-21.

Reeburgh WS., Ward BB., Whalen SC., Sandbeck KA., Kilpatrick KA., Kerkhof LJ. 1991. Black Sea methande geochemistry. Deep-Sea Research, Part A 38: S1189-210.

Ross DA., Degens ET., MacIlvaine J. 1970. Black Sea: Recent Sedimentary History. Science 170: 163-5.

Roepert A. 2014. Reconstructing Holocene environmental conditions at a site on the Western Black Sea continental slope using high-resolution geochemical records of sediment cores. MSc Thesis, Utrecht university. p. 96

Ruttenberg KC. 1992. Development of a Sequential Extraction Method for Different Forms of Phosphorus in Marine Sediments. Limnology and Oceanography 37: 1460-82.

Ruttenberg KC. and Berner RA. 1993. Authigenic apatite formation and burial in sediments from non-upwelling, continental margin environments. Geochimica et Cosmochimica Acta 57: 991-1007.

Ruttenberg KC. and Sulak DJ. 2011. Sorption and desorption of dissolved organic phosphorus onto iron (oxyhydr)oxides in seawater. Geochimica et Cosmochimica Acta 75: 4095-112.

Scholz F., Servermann S., McManus J., Hensen C. 2014. Beyond the Black Sea paradigm: The sedimentary fingerprint of an open-marine iron shuttle. Geochimica et Cosmochimica Acta 127: 368-80.

Shaffer G. 1986. Phosphate pumps and shuttles in the Black Sea. Nature 321: 515-7.

Sivan O., Adler M., Pearson A., Gelman F., Bar-Or I., John SG., Eckert W. 2011. Geochemical evidence for iron-mediated anaerobic oxidation of methane. Limnology and Oceanography 56: 1536-44.

Slomp CP., Thomson J., De Lange GJ. 2002. Enhanced regeneration of phosphorus during fromation of the most recent eastern mediterranean sapropel (S1). Geochimica et Cosmochimica Acta 66: 1171-84.

Tyrell T. 1999. The relative influences of nitrogen and phosphorus on oceanic primary production. Nature 400: 525-31.

Wijsman JWM., Middelburg JJ., Heip CHR. 2001. Reacitve iron in Black Sea Sediments: implications for iron cycling. Marine Geology 172: 167-80.